On the zenith hydrostatic delay for GPS measurements in Egypt: assessments of available prediction models

Ashraf El-kutb Mousa
National Research Institute of Astronomy and Geophysics, Helwan, Cairo, Egypt

Correction for the delay of an electromagnetic wave as it traverses the neutral atmosphere is the dominant error source for high precision geodetic GPS measurements. The delay is conveniently divided into two components, which have been designated the hydrostatic and wet components of the atmospheric delay. For the prediction of the zenith value of these two parameters several models have been proposed. The hydrostatic delay can be predicted with high accuracy. However, these models have not been tested for the Egyptian climate conditions. This paper uses Ray-tracing method for testing the available hydrostatic delay models. Nine sites representing the different conditions in Egypt are used to test Saastamoinen, Davis, Hopfield and Baby hydrostatic delay models. The results show that the Hopfield model is the best model among the available models for the nine sites. However, all the models, including Hopfield do not satisfy the requirements of precise geodetic application such as crust deformation studies.

يعتبر التباطؤ الحادث للموجات الكهرومغناطيسيه نتيجة لمرورها في الجزء المتعادل من الغلاف الجوى هو مصدر الخطأ الرئيسي المؤثر علي القياسات الجيوديسية الدقيقة باستخدام نظام GPS. و عموما يقسم هذا التباطؤ الى مركبتان هما المركبة الجافة و المبتلة. و للتنبؤ بقيمة كل من هاتان المركبتان فى الاتجاه الرأسي توجد مجموعة من النماذج المقترحة. وعموما يمكن حساب المركبة الجافة بدقة عالية. ولكن هذه النماذج لم تختبر صلاحيتها بالنسبة لمصر.البحث الحالي يستخدم طريقة تتبع الشعاع العددية لاختبار النماذج التي تتنبأ بالمركبة الجافة. تم اختيار تسعة مواقع لتمثل الظروف المختلفة في مصر و ذلك لإختبار النماذج التي أعدها كل من Saastamoinen و Hopfield و Davis. وقد أظهرت النتائج أن نموذج Hopfield كان أفضل هذه النماذج على الاطلاق. وعلى الرغم من ذلك فإن كل النماذج بما فيها Hopfield لم تحقق شروط الدقة المطلوبة لتطبيقات الجيوديسيا الدقيقة مثل دراسات تشوهات القشرة الأرضية.

Keywords: Hydrostatic delay, Atmospheric delay, Ray-tracing method, Hopfield and baby models

1. Introduction

The propagation delay induced by the electrically neutral atmosphere has been recognized as the most problematic modeling error for radiometric space geodetic techniques; such as GPS and VLBI. A wrong modeling of this delay affects significantly the height component of the position [1]. This delay is therefore a matter of concern in space-geodesy applications, such as crust deformation studies and sea level monitoring.

The neutral atmosphere propagation delay is commonly considered as composed of two components: a hydrostatic component and a wet component. Each one can be described as the zenith and a mapping function, which models the elevation dependence of the delay [2]. Several models have been proposed to account for both the zenith delay as well as the mapping function in the global scale, see for details [3-9].

This paper discusses the accuracy of the Saastamoinen, Davis, Hopfield and Baby zenith hydrostatic delay models for the Egypt climate. This performance evaluation is based on a comparison against 108 benchmark values, obtained by a ray tracing one year of atmospheric profiles for nine stations distributed all over Egypt. In this study, the accuracy of the tested model was evaluated in terms of its bias, and Root Mean Square (RMS) scatters.

2. Basic theory

A radio wave propagating through the earth's atmosphere, encounters variation in the atmospheric refractivity along its trajectory. This changes the propagation speed and bends the ray path. The atmospheric

delay (ΔL), along the actual path traveled by the radio wave is [10],

$$\Delta L = \int_s n\,ds - L_G. \quad (1)$$

Where n is the refractive index of the moist air, S is the actual path traveled, and G is the straight-line path from the satellite to the receiver point. It is more numerical stable to express the above integral in terms of refractivity [11]. Refractivity (N) is given as:

$$N = (n-1) * 10^{-6}. \quad (2)$$

Using eq. (2), the delay ΔL is formulated as:

$$\Delta L = 10^{-6} \int_s N\,ds + (L_S - L_G). \quad (3)$$

Where, the integration is along *S* (i.e., the actual path traveled). The first term in the right hand side of eq. (3) is the refractivity error, while the last term represents the geometric range error, the difference in length between the straight line G and the curved path *S*.

The radio refractivity of the neutral atmosphere is central to all theories concerning the radio waves propagation through the neutral atmosphere. The classic expression for the radio refractivity is [12],

$$N = k1\frac{Pd}{T} + k2\frac{Pw}{T} + k3\frac{Pw}{T^2}. \quad (4)$$

Where Pd, and Pw are the partial pressures of the dry gases and water vapor respectively, in mbar, and T is the absolute temperature in Kelvin. Several attempts have been made to calculate the constants k1, k2 and k3. Their values are available in many references [13, 14].

The first term of the right hand side of eq. (4) represents the dry part of refractivity, while the last two terms are the wet part. Using the equation of state of air, [5] presented a more compact form for refractivity,

$$N = k1R_d\rho + k2'\frac{Pw}{T} + k3\frac{Pw}{T^2}, \quad (5)$$

where ρ is the total mass density of the air, and k2' is a modified version of k2. The first term of the right hand side of eq. (5) is called the hydrostatic refractivity, while the other two form the wet refractivity. It is important here to understand the difference between eqs. (4, 5). Since in eq. (5), a part of the water vapor influence has been absorbed in the hydrostatic delay. Throughout the current paper, the two terms hydrostatic and dry will be used interchangeably, but the meaning refer to the hydrostatic definition. As the rest of the paper evaluate only the hydrostatic delay models, now the hydrostatic delay (ΔL_h) can be written as;

$$\Delta L_h = 10^{-6} \int k1 R_d \rho\,ds. \quad (6)$$

2.1. *Hydrostatic zenith delay models*

Using eq. (6), the hydrostatic delay in the zenith direction (ΔL^z_h) is obtained by replacing path elements ds with the vertical elements dz

$$\Delta L^z_h = 10^{-6} \int k1 R_d \rho\,dz. \quad (7)$$

It is possible to perform the integration in eq. (7) if we apply the condition that hydrostatic equilibrium is satisfied, i.e.

$$dp/dz = -\rho(z)\,g(z). \quad (8)$$

Where g(z) is the acceleration due to gravity at the vertical coordinate z, P(z) is the total pressure.

$$\Delta L^z_h = 10^{-6} k1 R_d \frac{Ps}{gm}. \quad (9)$$

Where, gm is the mean gravity acceleration and Ps is the surface pressure.

The modeling of the zenith hydrostatic delay is therefore straightforward, and models can only differ due to the choice of the refractivity constant (k1) and on modeling of the height and latitude dependence of the

gravity acceleration. Based on this theoretical approach, models were developed by [4] -later modified by Davis et al. [5]- and Baby et al. [8]. Hopfield developed her model for zenith dry delay based on the quartic refractivity profile. A brief summary of these models is given below.

2.2. Saastamoinen model

Saastamoinen [4] found that gm could be expressed (in ms^{-2}) as:

$$gm = 9.784(1-0.0026\cos 2\phi - 2.8\times10^{-7}Hs). \quad (10)$$

Where ϕ is the latitude of the station and Hs is the station height above sea level, in meters. He used the refractivity constant given by Essen and Froome [15]. Using eq. (10) and substitute in eq. (9), he obtained;

$$\Delta L_h^z = \frac{0.00277P_s}{(1-0.0026\cos 2\varphi - 2.8\times10^{-7}Hs)}. \quad (11)$$

2.3. Davis et al;

Davis et al. [5] used the k1 refractivity constant given by Thayer [14], and improved Saastamoinen model as;

$$\Delta L_h^z = \frac{0.0022768Ps}{(1-0.0026\cos 2\varphi - 2.8\times10^{-7}Hs)}. \quad (12)$$

2.4. Baby et al;

Baby et al. [8] suggested that the gravity acceleration be expresses as;

$$gm = \frac{gs}{1+\frac{2}{rs\sigma(\mu+1)}} \quad (13)$$

In the above equation, gs is the surface gravity at the used station,

$$\mu = \frac{gs}{R_d\alpha}(1-\frac{2}{rs\sigma}), \quad (14)$$

$$\sigma = \alpha/Ts, \quad (15)$$

where α is the temperature lapse rate and rs is the geocentric radius of the station, in metes. Combining eqs. (10) and (13) and using the refractivity constant K1 as given by Bean and Dutton [12], they obtained;

$$\Delta L_h^z = \frac{0.002277Ps}{gs}(1+\frac{2}{rs\sigma(\mu+1)}) \quad (16)$$

2.5. Hopfield model

Hopfield [6] was followed a different strategy. She assumed that the theoretical dry refractivity profile could be expresses by the quartic model;

$$N_d = N_{ds}\frac{(H_d^e - H)^4}{(H_d^e)^4} \quad (17)$$

Where H_d^e is the dry equivalent height, which is given as Hopfield [16];

$$H_d^e = 40.136 + 0.14872\,ts. \quad (18)$$

Where ts is the station surface temperature in ^oC.

Substitution of eq. (17) into eq. (10) and integration results in,

$$\Delta L_h^z = 77.6\times\frac{Ps}{Ts}\times\frac{H_d^e}{5}. \quad (19)$$

3. Data analysis

Nine station distributed all over Egypt are used for testing the performance of the four models stated above. These stations are chosen to represent different climate conditions. They are also mostly distributed evenly to cover Egypt as seen in fig. 1. Moreover, their locations are chosen in active areas where precise geodetic network are established for crust movement studies. The station coordinates are listed in table 1. For every station, the monthly average values of the meteorological parameters are used. This results in 108-test point for every model.

The MSIS model [17] is used to provide the vertical profiles of temperature and pressure that is needed for the ray tracing analysis. The average monthly value of the temperature and pressure are used. Ray tracing is the process of determining the path of an electromagnetic signal, based on geometric optics theory applied over a series of thin spherical shells, concentric with the earth, and within which a constant refractivity is assumed [13, 18, 19]. For the current analysis, layer thickness of 100 ms is used.

Ray tracing is carried out numerically to integrate eq. (10). The results of the ray tracing are considered the benchmark against which the models are tested. As a rule, the models were tested using the standard formulation specified by the authors as summarized above. For the sake of simplicity, the models will be named in the text after the author abbreviated as Saas for Saastamoinen, Dav for Davis et al., Hop for Hopfield, and Baby_88 for Baby et al. All Models are driven by the values of the MSIS model at their respective heights.

The accuracy of a model will be evaluated in terms of its bias, and RMS scatter. The bias corresponds to the difference between the predicted values given by the model and the ray traced values. The RMS scatter corresponds to the standard deviation of the differences about the mean value.

4. Results and discussion

Figs. 2 through 10 show the result of the assessment for individual station. A through investigation of these figures reveals the following results. It is clear that Hop model shows the least error for all the stations and months. Hop models always overestimate the delay by about 1-3 mm. Baby_88 model always underestimate the delay by about 4-15 mm. Generally, both Saas and Dav underestimate the delay by about 4-8 mm,

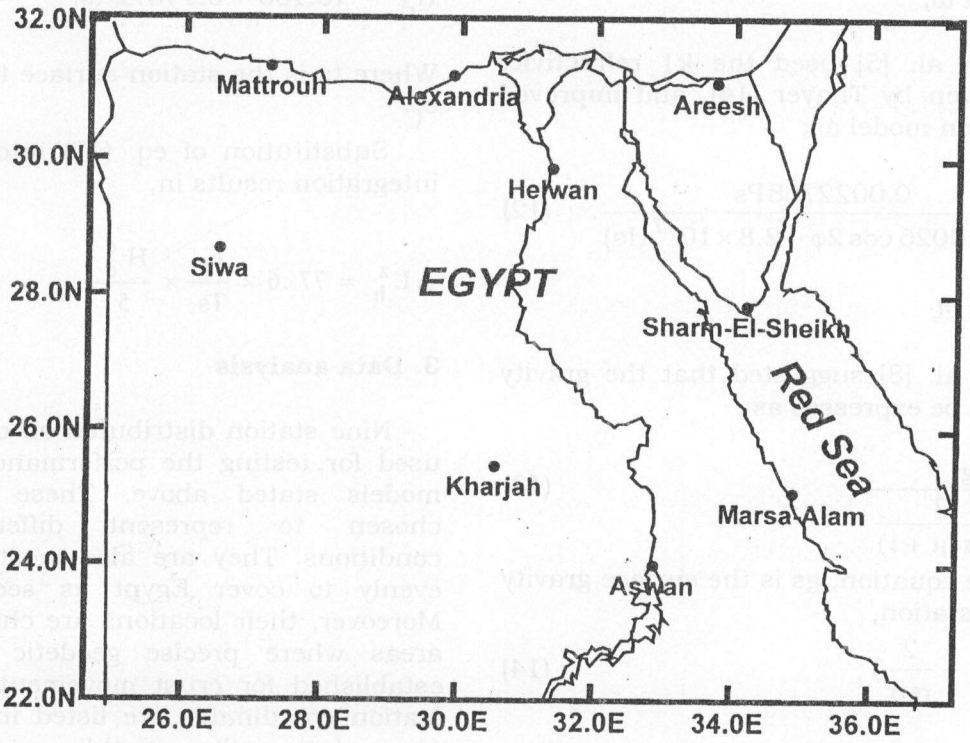

Fig. 1. Map showing the location of the nine sites all over Egypt used in this study.

except for Alexandria, fig. 3, Kharjah, fig. 10, and Mersa-Alam fig. 8, where the overestimate the delay by about 1-2 mm.

It is interesting to note that for Alexandria fig. 3, Kharjah, fig. 10, and Mersa-Alam, fig. 8, Saas, Dav as well as Hop models show very close results. For Aswan, fig. 9, both Saas and Dav show their highest error of about 10-12 mm. Hop shows its best result at Aswan (Fig. 9) with error of about 0.4 mm. For Baby_88, except for Alexandria, fig. 2, and Mersa-Alam, fig. 8, the errors were in the range of 10 mm. For Alexandria, fig. 2, and Mersa-Alam, Baby_88 shows its best results with an error of about 4-6 mm.

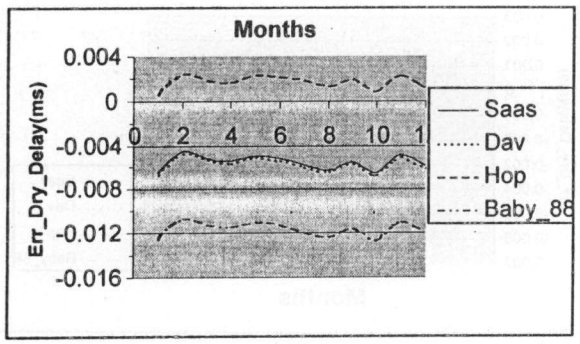

Fig. 2. Zenith dry delay models error for one year at Areesh City, Northeastern Egypt.

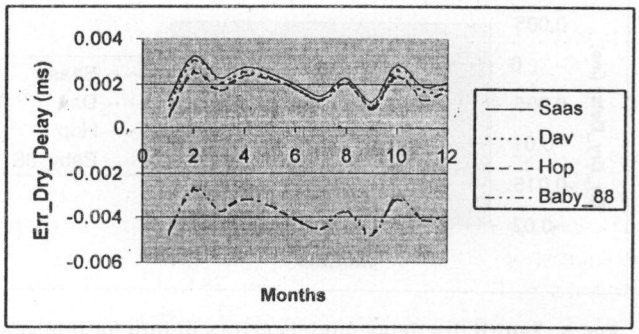

Fig. 3. Zenith dry delay models errors in mm for one year at Alexandria, Northern Egypt.

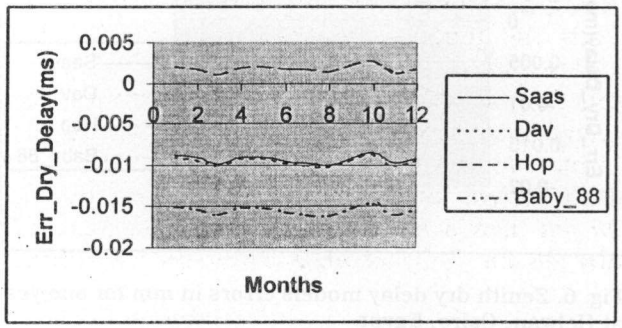

Fig. 4. Zenith dry delay models errors in mm for one year at Mattroah, Northwestern Egypt.

Table 1
The coordinates of sites used in the present analysis

Site name	Latitude (degree)	Longitude (degree)	Height (meter)
Areesh	31.11802	33.71026	35.4789
Alexandria	31.21264	29.88460	29.3432
Mattrouh	31.34557	27.23088	57.9610
Sharm El-Sheikh	27.84643	34.183750	257.0900
Helwan	29.86191	31.344364	146.170
Siwa	28.67216	26.510377	18.6000
Marsa Alam	25.066813	34.878075	43.8270
Aswan	24.00198	32.869000	186.950
Kharjah	25.451694	30.542361	96.3000

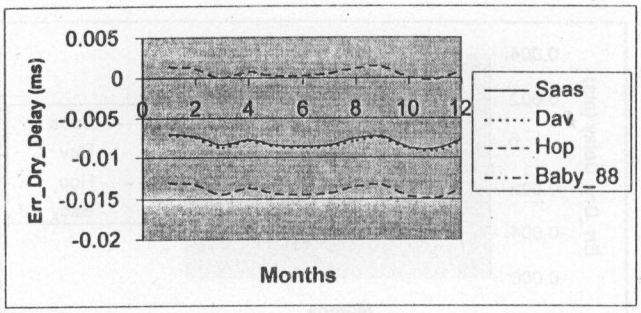

Fig. 5. Zenith dry delay models errors in mm for one year at Sharm El-Sheik, Sinai, Northeastern, Egypt.

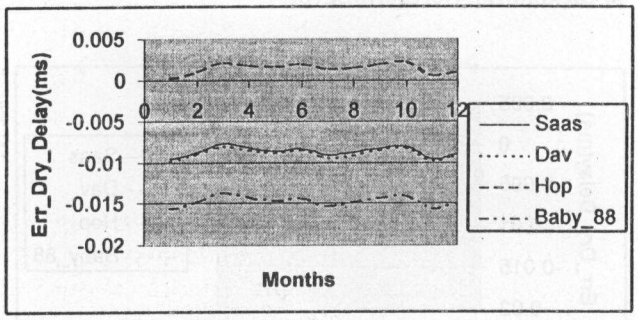

Fig. 6. Zenith dry delay models errors in mm for one year at Helwan, Cairo, Egypt.

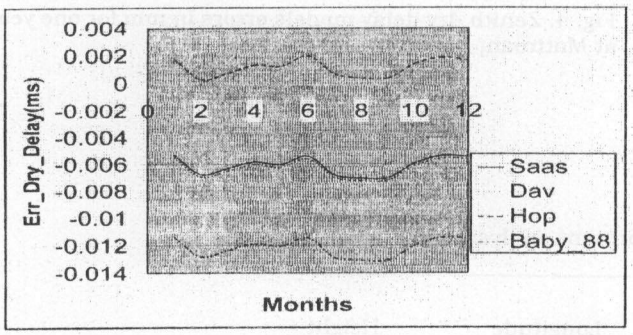

Fig. 7. Zenith dry delay models errors in mm for one year at Siwa, Western Desert, Egypt.

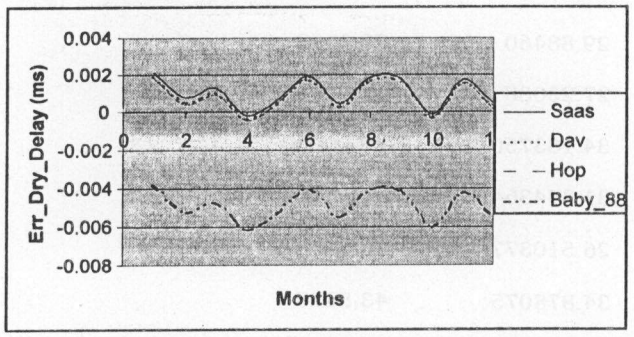

Fig. 8. Zenith dry delay models errors in mm for one year at Marsa-Alam, Red Sea Coast Egypt.

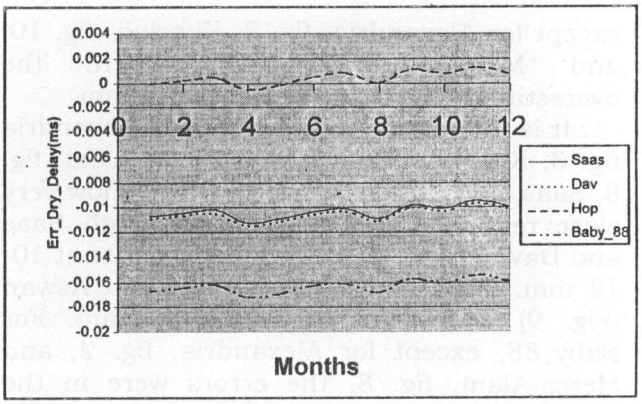

Fig. 9. Zenith dry delay models errors in mm for one year at Aswan, Southern Egypt.

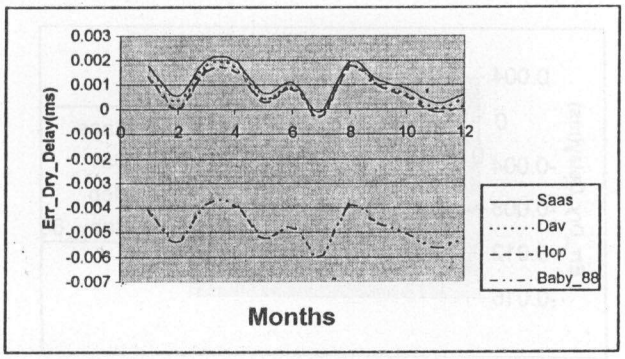

Fig. 10. Zenith dry delay models errors in mm for one year at Kharjah, Western Desert, Egypt.

Table 2 shows the yearly average biases of the models for the nine stations as well as the RMS scatter around that mean bias. Hop model is the best over all with biases in the range of 0.4-2 mm. On the other hand, Baby-88 gives the highest biases (about 5- 15 mm). The range of biases for both Saas and Dav is the middle range (2-10 mm). All the models show the same range of rms. The values are in the range of 0.0004–0.0008. Hop model shows marginally smaller values.

To address topics of current geophysical interest, such as crust deformation, sea surface monitoring, 1.0 mm horizontal accuracy and 3.0 mm vertical accuracy is needed [20]. On the other hand, Niell [21], Herring [22], and MacMillan and Ma [23] have shown that the error in the vertical coordinate is approximately one third of the error in the propagation delay. Thus if we consider the minimum elevation angle to be 5°, the error of

Table 2
Mean errors (meters) and the RMS of the tested zenith dry delay models

Model	Saas.		Dav.		Hop.		Baby_88	
City	Mean	RMS	Mean	RMS	Mean	RMS	Mean	RMS
Areesh	-5.52E-03	0.000657	-5.72E-03	0.000657	1.73E-03	0.000643	-1.16E-02	0.00066
Alexandria	2.13E-03	0.000653	1.93E-03	0.000653	1.72E-03	0.000648	-3.83E-03	0.000654
Mattrouh	-9.29E-03	0.000481	-9.50E-03	0.000481	1.87E-03	0.000472	-1.54E-02	0.00048
Sharm	-7.97E-03	0.000627	-8.17E-03	6.27E-04	6.68E-04	6.03E-04	-1.39E-02	6.25E-04
Helwan	-8.65E-03	0.000584	-8.85E-03	0.000584	1.49E-03	0.000626	-1.47E-02	0.000593
Siwa	-6.11E-03	0.000675	-6.31E-03	0.000674	1.14E-03	0.00062	-1.22E-02	0.000673
Marsa Alam	1.07E-03	0.000834	8.69E-04	0.000834	8.58E-04	0.000856	-4.87E-03	0.000837
Aswan	-1.03E-02	0.000524	-1.05E-02	0.000524	4.67E-04	0.000551	-1.63E-02	0.000522
Kharjah	1.07E-03	0.000715	8.74E-04	0.000715	7.33E-04	0.000707	-4.80E-03	0.00072

the delay at this elevation angle should be better that 10 mm. Simple calculations show that the hydrostatic delay error at zenith should be in the sub-millimeter level. However, our assessment showed that even Hop model gives error of few millimeters. Thus a new local model for the Egypt conditions should be designed and used. This point will be study in the future work.

5. Conclusions

An assessment analysis of the hydrostatic delay models at the zenith has been tested in the present study for the Egyptian climate. Nine stations mostly evenly distributed all over Egypt are used. The Saastamoinen, Davis, Hopfield and Baby models have been tested by a ray tracing of data against MSIS model, which was used as a reference. This analysis indicated that Hopfield model gives the smallest errors and the best performance among these models. Hopfield model errors are in the range of 1-3 mm. On the other hand, Baby-88 model shows the worst results with errors in the range of 10-16 mm. Both Saastamoinen and Davis models show similar performance with about 5-9 mm errors. However, the estimated accuracy of all the tested hydrostatic delay models, including Hopfield model, do not meet the requirements of the current precise geodetic applications in Egypt such as crust movements monitoring and monitoring of sea level. Thus it is recommended to design a local model for prediction of the delay at the zenith. The accuracy of the thought model should be within the sub-millimeters level. This is left to be studied in details in a future analysis.

References

[1] A. H. Dodson, P.J. Shardlow, L.C.M. Hubbard, G. Elgered, and P.O.J Jarlmark "Wet Tropospheric Effects on Precise GPS Height Determination", Journal of Geodesy, Vol. 70, pp. 188-202 (1996).

[2] A. K. Mousa, "Characteristics of Wet Tropospheric Delay Deduced From Water Vapor Radiometer Data and Their Implications for GPS Baseline Solution Accuracy." Ph.D Thesis, Graduate School of Science, Kyoto University, Kyoto, Japan (1997).

[3] J. Saastamoinen, "Atmospheric Correction for the Troposphere and Stratosphere in Radio Ranging of Satellites." in The Use of Artificial Satellites for Geodesy (S. W. Henriksen et al, eds.), Geophysics Monograph Series, Vol. 15, pp. 274-251 (1972).

[4] J. Saastamoinen, "Contributions to the Theory of Atmospheric Refraction." in three parts. Bulletin Geodesique, No. 105, pp 278-298; No. 106, pp. 383-397; No. 107, pp 13-34 (1973).

[5] J. L. Davis, T.A. Herring, I. I. Shapiro, A. E. E. Rogers, and G. Elgered, "Geodesy by

Radio Interferometry Effects of Atmospheric Modeling Errors on Estimates of Baseline Length." Radio Science, Vol. 96 (B1), pp. 643-650 (1985).

[6] H. S. Hopfield "Two-Quadratic Tropospheric Refractivity Profile For Correcting Satellite Data." Journal of Geophysical Research, Vol. 74 (18), pp. 4487- 4499 (1969).

[7] H. S. Hopfield "Tropospheric Effect on Electromagnetically Measured Range: Prediction From Surface Weather Data." Radio Science, Vol. 6 (3), pp. 357- 367 (1971).

[8] H.B. Baby, P. Gole, and J. Laverbnat "A Model For The Tropospheric Excess Path Length of Radio Waves From Surface Meteorological Measurements" Radio Science, Vol. 23, pp. 1023- 1038 (1988).

[9] A. E. Niell "Global Mapping Function for the Atmospheric Delay at Radio Wavelengths." Journal of Geophysical Research, Vol. 101 (B2), pp. 3227-3246 (1996).

[10] V. B. Mendes "Modeling the Neutral-Atmospheric Propagation Delay in Radiometric Space Techniques." Ph. D. Dissertation, Department of Geodesy and Geomatics Engineering Technical Report No. 199, University of New Brunswick, Fredericton, New Brunswick, Canada (1999).

[11] J. L. Davis " Atmospheric Propagation Effects on Radio Interferometry" Ph. D. Dissertation. Air Force Geophysics Laboratory Technical Report AFGL- TR-86-0243, Hanscom AFB, MA (1986).

[12] E. K. Smith, and S. Weintraub "The Constants in the Equation of Atmospheric Refractive Index at Radio Frequencies." Proceedings of the Institute of Radio Engineers, Vol. 41 (8), pp. 1035-1037 (1953).

[13] B. R. Bean and E.J. Dutton "Radio Meteorology." National Bureau of Standards Monograph 92, U.S. Government Printing Office, Washington, D.C. (1966).

[14] G. D. Thayer " An Improved Equation for the Radio Refractive Index of Air." Radio Science, Vol. 9 (10), pp. 803-807 (1974).

[15] L. Essen and K.D. Froome "The Refractive Indices and Dielectric constants of Air and its Principal Constituents at 24,000 Mc/s." Proc. Royal Soc. B, Vol. 64, pp. 862-875 (1951).

[16] H. S. Hopfield "Tropospheric Refraction Effects on Satellite Ranging Measurements." APL Technical Digest, Vol. 11 (4), pp. 11-21 (1972).

[17] A. E. Hedin "Extension of the MSIS Thermosphereic Model into Middle and Lower Atmosphere." JGR, Vol. 96 (A2), pp. 1159-1172 (1991).

[18] D. E. Kerr "Propagation of Short Radiowaves." (Ed.) McGraw-Hill, New York (1953).

[19] P. A. Bradly "Propagation of Radiowaves in the Ionosphere." In Radiowave Propagation." M.P.M. Hall and L. W. Barclay (Eds.), IEEE Electromagnetic Waves Series, Peter Peregrinus Ltd. On behalf of the Institute of Electrical Engineers, London (1989).

[20] J. X. Mitrovica, J. L. Davis and I. I. Shapiro "A Spectral Formalism for Computing Three-Dimensional Deformations Due to Surface Loads, 2, Present-Day Glacial Isostatic Adjustment." Journal of Geophysical Research, Vol. 99 (B4), pp. 7075-7101 (1994).

[21] A. E. Niell "Vertical Change and Atmosphere correction in VLBI" in AGU Chapman Conference Proceedings on Geodetic VLBI: Monitoring Global Change, NOAA Technical Report NOS 137 NGS 49, pp. 147- 158 (1991).

[22] T. A. Herring "Modeling Atmospheric Delays in the Analysis of Space Geodetic Data", Symposium of Transatmospheric Signals in Geodesy, Netherlands Geod. Commis. Ser. 36, Ned. Comm. Voor Geod., Delft, pp. 157-164 (1992).

[23] D. S. MacMillan and C. Ma "Evaluation of Very Long Baseline Interferometry Atmospheric Modeling Improvements." Journal of Geophysical Research, Vol. 99 (B1), pp. 637-651 (1994).

Received March 28, 2002
Accepted May 11, 2002